Journal of Sol-Gel Science and Technology (2018) 85:638–646
https://doi.org/10.1007/s10971-018-4596-z

ORIGINAL PAPER: NANO-STRUCTURED MATERIALS (PARTICLES, FIBERS, COLLOIDS, COMPOSITES, ETC.)

Natural clay attapulgite as the raw material for synthesis of Al/Ti/Mg-containing mesoporous silicates with cubic, 3D hexagonal, and lamellar mesostructures

Bing Guo[1] · Xiuzhen Lin[1,2] · Zhongyong Yuan[2]

Received: 8 December 2017 / Accepted: 22 January 2018 / Published online: 14 February 2018

Abstract

A series of Al/Ti/Mg-containing ordered mesostructured silicates were synthesized using the natural attapulgite clay as the raw material, which was first pretreated by 4 M hydrochloric acid without other special treatment such as grinding. By varying the pH value in the synthetic gel, different mesophases with cubic, 3D hexagonal, and lamellar mesostructures were obtained. Their mesostructures were confirmed by low-angle X-ray diffraction (XRD) and transmission electron microscopy (TEM). Their morphology and textural properties were analyzed by scanning electron microscopy (SEM) and N_2 adsorption. It was found that the hetero-atoms including Al, Ti, and Mg in the clay could be effectively transformed into these ordered mesostructured silicate frameworks in sufficient content, as revealed by inductively coupled plasma (ICP) emission spectroscopy and fourier transform infrared (FT-IR) spectrum. NH_3-TPD showed the accessibility of Al species as Brönsted and Lewis acid sites in the mesostructured framework located on the pore surface. All above suggests the potential of attapulgite as a low-cost precursor for the industrial scale production of high quality heteroatom-doped mesophases for various applications. Low-angle powder X-ray diffraction patterns of mesostructured silicates with cubic, 3D hexagonal, and lamellar mesophases, synthesized by using natural clay attapulgite as raw material: uncalcined (left) and calcined (right).

Graphical Abstract

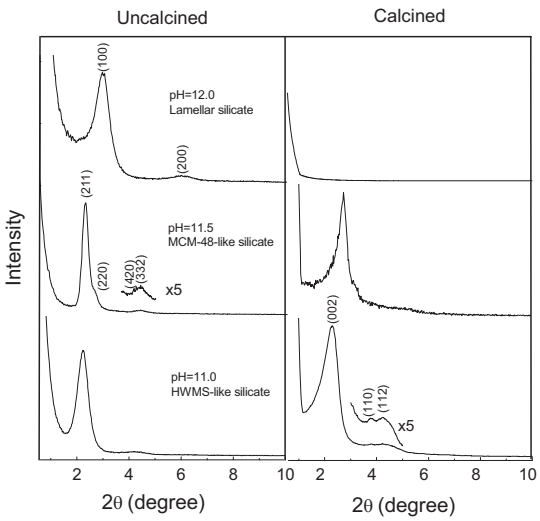

✉ Xiuzhen Lin
xiuzhen_lin@126.com

[1] School of Environment and Civil Engineering, Dongguan University of Technology, Dongguan, Guangdong 523808, China

[2] Institute of New Catalytic Materials Science, Key Laboratory of Advanced Energy Materials Chemistry (Ministry of Education), College of Chemistry, Nankai University, Tianjin 300071, China

Keywords Attapulgite · Cubic silicates · Hexagonal silicates · Lamellar silicates

Highlights

- Cubic, 3D hexagonal, and lamellar silicates have been synthesized with attapulgite as raw material.
- It is essential to pretreat natural clay attapulgite (APT) via acid leaching step.
- The content of metal ions including Al, Ti, Mg can be well preserved in acid-activated APT.
- Those metal ions can be well transferred into ordered mesoporous silicates in desirable content.
- The mesophases of silicates can be fabricated by controlling pH value in the synthetic step.

1 Introduction

Mesostructured molecular sieves, in particular the M41S family, owing to its high surface area and uniform pore structure with the ability to select its pore size, make them very promising as catalysts, catalyst supports, and adsorbents [1–4]. However, the pure siliceous mesoporous materials due to the absence of active sites in their neutral frameworks are of limited use as catalysts. Incorporation of hetero-atoms into the framework sites is a favorable way to provide these materials with potential applications for heterogeneous catalysis, photocatalysis and ion-exchange [5–8]. Up to now, attempts to incorporate single transition metal such as Al, Ti, Fe, Zr, V, or Mn, and binary or ternary metal ions into MCM-48 [9–11], MCM-41 [12–14], and HMS [15] have been reported. The integration of binary or ternary metal ions into mesoporous molecular sieves not only has the effect that single metal worked, but also can work cooperatively to exhibit higher efficiency [16, 17]. Therefore, undoubtedly the integration of multiple metal species to siliceous mesostructured materials would provide multifuntionalities and extensively expand their applications. Besides, the incorporation of foreign metal cations into siliceous mesostructure via extra addition of them in preparation stage currently was an efficient and main strategy.

Considering the requirements on the economy and environmental protection issues in industry, silicon alkoxides as the silicon source commonly used to synthesize mesoporous molecular sieves, were the primary target to be replaced due to their expensiveness and polluting environment, and the extra addition of doped metals into them also increased the cost and complicated the preparation procedure. Jang et al. [18] prepared highly siliceous MCM-48 from rice husk ash, which was first transformed into sodium silicate solution under alkaline pretreatment. Kumar et al. [19] prepared Al-MCM-41 using the supernatant of the coal fly ash as the silicon and aluminum source by pretreatment of the starting material under alkaline condition as well. The natural clay, metakaolin was also used to produce hexagonal, cubic and wormhole aluminosilicate by pretreated the clay first transferred into faujasitic zeolite nanoclusters as precursor under alkaline conditions [20]. To utilize the cost-free materials such as ash and clays rich in silicon and metal elements as Si and metal sources would be a desirable alternative to synthesize metal-doped mesostructured silicates. In particular, the clays containing plentiful silicon and various metal elements (Mg, Al, Fe, and Ti), would both decrease the cost largely and reduce harm to the environment.

Attapulgite (APT, or palygorskite as it often called), characteristic of a porous crystalline structure containing SiO_4 tetrahedral layers alloyed together along longitudinal sideline chains consisting of octahedral cations like Al, Fe, and Mg, is existed in the nature widely. Its common chemical formula can be written as $[(H_2O)_4(Mg, Al, Fe)_5(OH)_2Si_8O_{20}{\cdot}4H_2O]$ and the amount of other metal compositions like Ti and Mn in small quantity is different depending on the places they are mined. Yang et al. [21] have reported the synthesis of Al-MCM-41 from natural attapulgite without addition of silica or aluminum reagents with a pretreatment process involving sequential mechanical grinding and 8 M acid leaching at 80 °C for 2 h. They found that the mechanical grinding of attapulgite resulting in amorphization and partial structural breakdown is critical to the successful synthesis of Al-MCM-41. In this paper, we synthesized a series of Al/Ti/Mg-doped mesostructured silicates including cubic *Ia3d*, three-dimensional (3D) hexagonal *P6mmm* and lamellar silicates by using attapulgite as the raw material, which was first pretreated under 4 M HCl at 90 °C for 3 h directly without mechanical grinding, and followed by hydrothermal synthesis in the presence of surfactant cetyltrimethylammonium bromide as the template.

2 Experimental section

2.1 Materials

The natural attapulgite clay was obtained from Anhui Tianjiao Corp., and its chemical composition was 58.23–66.30% of SiO_2, 10.50–11.90% of Al_2O_3, 8.10–12.65% of MgO, 5.80–6.51% of Fe_2O_3, 0.76–1.10% of TiO_2, 0.008–0.15% of Mn_2O_3, 0.68–0.91% of K_2O, 0.29–4.15% of CaO, and 0.02–0.13% of MnO.

Cetyltrimethyl ammonium bromide (CTAB) and tetraethyl orthosilicate (TEOS) were obtained from Tianjin Guangfu Fine Chemical Co. Ltd. Sodium hydroxide and absolute ethanol were provided by Tianjin Yingda Rare Chemical Reagent Corp.

2.2 The pretreatment of attapulgite clay

Typically, the attapulgite clay (denoted as APT, 3.0 g) was pretreated with 4 M HCl (150 ml) at 90 °C for 3 h, and cooled to room temperature. The suspension was filtered, thoroughly washed with deionized water to remove Cl^- and dried at 80 °C for 5 h. The obtained acid-leached active powder (denoted as HAPT) was used as silicon and hetero-element sources directly to prepare multi-metal-doped mesostructured silicates.

2.3 Synthesis of cubic Ia3d silicate, lamellar silicate, and 3D hexagonal wormhole-like silicate

For the synthesis of well-ordered cubic *Ia3d* silicate (denoted as MCM-48-like silicate), CTAB was used as the structure directing agent with extra addition of ethanol. Typically, HAPT (0.9 g) was added into a mixture of deionized water (20 ml), ethanol (2 ml), and CTAB (2.5 g). Then, 2 M sodium hydroxide solution was added dropwise to adjust the pH value to 11.5. The mixture was stirred at 70 °C for 3 h in order to get the homogeneous gel, then transferred into a Teflon-lined steel autoclave and statically heated at 110 °C for 24 h. The resultant products were filtered, washed repeatedly with deionized water and dried overnight at 80 °C. Subsequently, the as-prepared samples were calcined at 550 °C for 6 h in air with a heating rate of 2 °C/min to obtain surfactant-free silicate powder. Pure MCM-48 was prepared with TEOS as the silicon source and the molar composition of the initial gel mixture was $1{:}0.23{:}0.55{:}112SiO_2/Na_2O/CTAB/H_2O$.

Three-dimensional (3D) Hexagonal wormhole-like mesostructured silicate (denoted as WHMS-like silicate), and lamellar silicate were obtained under the same procedure as the preparation of MCM-48-like silicate just adjusting the pH values to 11.0 and 12.0, respectively.

2.4 Preparation of H-MCM-48-like silicate and H-WHMS-like silicate

The protonated form of MCM-48-like and WHMS-like silicates (correspondingly denoted as H-MCM-48-like and H-WHMS-like silicates) were prepared from the calcined samples by ion-exchange. MCM-48-like and WHMS-like silicates were first treated by repeated exchange of the calcined samples with 1 M NH_4NO_3 solution at 80 °C for 6 h, followed by deammoniation at 550 °C for 6 h in air.

2.5 Sample characterization

X-ray diffraction (XRD) patterns were recorded on a Rigaku D/max-2500 diffractometer with CuK_α radiation operated at 40 kV and 100 mA. N_2 adsorption–desorption isotherms were recorded on a Quantachrome NOVA 2000e sorption analyzer at liquid nitrogen temperature (77 K). The samples were degassed at 200 °C for 5 h prior to the measurement. The surface area was calculated by the multi-point Brunauer-Emmett-Teller (BET) method and pore size distribution was calculated from the adsorption branch of the isotherms by the Barett-Joyner-Halenda (BJH) model. Scanning electron microscopy (SEM) and transmission electron microscopy (TEM) were carried out on a Shimadzu SS-550 microscope at 15 kV, and a Philips Tecnai G20 at 200 kV, respectively. FT-IR spectra were measured on a Bruker VECTOR 22 spectrometer with KBr pellet technique, and the ranges of spectrograms were 4000 to 400 cm^{-1}. The chemical compositions of Ti, Al and Mg were analyzed by inductively coupled plasma (ICP) emission spectroscopy on a Thermo Jarrell-Ash ICP-9000 (N + M) spectrometer. Diffuse reflectance UV–visible absorption spectroscopy was employed on a Shimadzu UV-2450 spectrophotometer over the wavelength range 200–800 nm, using $BaSO_4$ as a reference.

2.6 Temperature programmed desorption of ammonia

The acidity of H-MCM-48-like silicate and H-WHMS-like silicate was studied by temperature programmed desorption of ammonia (NH_3-TPD). About 200 mg of the sample was placed in a quartz reactor and was activated at 823 K in air for 6 h, followed by 2 h in helium with a flow rate of 20 ml/min. The reactor was then cooled to 373 K and maintained for another hour under the same condition. Ammonia adsorption was carried out by passing the gas through the sample for 30 min at this temperature. Subsequently, it was purged with helium for an hour to remove the physisorbed ammonia. Desorption of ammonia was carried out by heating the reactor up to 823 K at a uniform rate of 10 K/min. The amount of ammonia desorbed was estimated with the aid of thermal conductivity detector response factor for ammonia.

3 Results and discussion

3.1 APT pretreatment

Attapulgite clay was a kind of metal-rich silicate, mainly with SiO_2 weight of ~60 wt% and other metal oxides, particularly Al, Mg, Fe, and Ti in significant content.

Table 1 Elemental composition (wt%) of Si and metals, and the molar ratios of Si to metals in the calcined silicate materials

Sample designation	Si	Al	Ti	Mg	n_{Si}/n_{Al}	n_{Si}/n_{Ti}	n_{Si}/n_{Mg}
HAPT	29.72	0.98	0.34	0.25	29	150	101
WHMS-like silicate	34.09	1.77	0.74	0.27	19	79	108
MCM-48-like silicate	33.47	1.74	0.79	0.87	19	73	33
Lamellar silicate	30.69	1.57	0.29	0.19	19	181	138

HAPT being treated at 90 °C in 4 M HCl for 3 h

Therefore, APT was an ideal candidate as siliceous and foreign metal precursor for preparation of mesostructured silicates. Regrettably, the direct use of APT was unavailable. It was reported that alkaline environments affect the composition and the structure of minerals to a lesser extent than an acidic environment [22, 23]. Hence we pretreated the raw material in acidic solution. It was found that the acidic release of metal cations from APT was dependent on the pretreatment time, the concentration of pretreated HCl solution and temperature. For example, if we treated the APT in 8 M HCl for 8 h at 80 °C, almost all of the metal cations in the clay would be lost. And if the APT was treated with 1 M HCl for 8 h at 80 °C, most of metal cations could be left in the clay, but no mesostructured silicates can be fabricated by using 1 M HCl activated APT. In order to activate APT as well as preserve adequate metal cations, we arranged a series of experiments by varying the pretreatment factors. Ultimately, we found that the APT being treated at 90 °C in 4 M HCl for 3 h could be applied as precursor with desirable amount of metal cations. Under such treatment conditions, silicon species started to enrich in HAPT, whereas a large part of metal ions including Mg, Fe, Ti, and Al was dissolved into acid solution, and Mn and Ca almost can not be detected. ICP analysis showed the Al element was in 0.98 wt%, Mg in 0.25 wt%, and Ti in 0.34 wt% (see in Table 1). The wide-angle XRD showed the crystalline structure for HAPT was the same to APT with a little decrease in crystalinity, while an increase in quartz impurity at $2\theta = 26.7°$ was observed (in Fig. 1). TEM analysis showed the fiber-like structure after acid treatment still remained, as shown in Fig. 2. Interestingly the BET surface area of HAPT (264 m^2/g) doubled in comparison with that of APT (134 m^2/g) (Table 2).

3.2 Characterization of cubic Ia3d, 3D hexagonal, and lamellar silicates

HAPT obtained by activating at 90 °C in 4 M HCl for 3 h was adopted as the silicon and metal ions precursor. Followed by the addition of deionized water, CTAB and ethanol, the synthetic mixture was adjusted by 2 M NaOH to a pH value of 11.0. After stirring at 70 °C for 3 h, the homogeneous gel was transferred into a Teflon-lined steel autoclave and statically heated at 110 °C for 24 h. The finally prepared material was named as WHMS-like silicate. The low-angle XRD shown in Fig. 3 for the uncalcined WHMS-like silicate exhibited a main reflection at $2\theta = 2.25°$ and a wide diffraction peak in the range of 3.0–5.0°, characteristic of mesostructure but difficult to determine the exact mesophase due to the ill-resolved peak at high angle. Increasing the synthetic pH value to 11.5, cubic mesophase with *Ia3d* symmetry was obtained. The XRD pattern of the as-synthesized MCM-48-like silicate exhibited a sharp d_{211} Bragg reflection at $2\theta = 2.3°$, a weak d_{220} Brag reflection shoulder at $2\theta = 2.7°$ and several multiple peaks between 4° and 6°, which indicated the *Ia3d* bicontinuous cubic phase resembling as that of conventional siliceous MCM-48 from tetraethyl orthosilicate (TEOS) [24]. Further increasing the synthetic pH value to 12.0, only two peaks was observed at 3.0° and 6.0° (2θ), indexing to (100) and (200), respectively, which is consistent with the formation of a well-ordered lamellar material [25, 26]. Upon calcination, WHMS-like mesoporous silicate exhibited three reflections at 2.26, 3.77, and 4.24° (2θ) and calculated *d* spacings were found to agree well with the 3D hexagonal mesostructure. Unit cell parameters were $a = 4.68$ nm and $c = 7.81$ nm. The unit cell parameter ratio is $c/a = 1.67$, which is very close to the theoretical $c/a = 1.633$ for the hexagonal close-packed (hcp) phase. It means WHMS-like silicate have 3D hexagonal mesostructure. After combustion, MCM-48-like silicates induced lattice contraction of 18.7% with no significant effect on structural ordering, while the lamellar phase for lamellar silicate collapsed and the two peaks in the synthetic counterpart were not observed. Interestingly, as shown in Fig. 1, the calcined mesostructured silicates presented the amorphous framework, but with quartz left in the material. In comparison with HAPT, it could be found that the crystalline structure of HAPT was further destroyed upon treatment in alkaline synthetic system.

The TEM image of WHMS-like silicate in Fig. 4a, b gives wormhole-like mesostructure. In combination of XRD analysis, it can be concluded that WHMS-like silicate had a 3D hexagonal and wormhole-like mesostructure. In Fig. 4c, d, MCM-48-like silicate for selected particles along the (100) and (110) directions was presented, which matched well with the reported MCM-48 images [27]. Along the

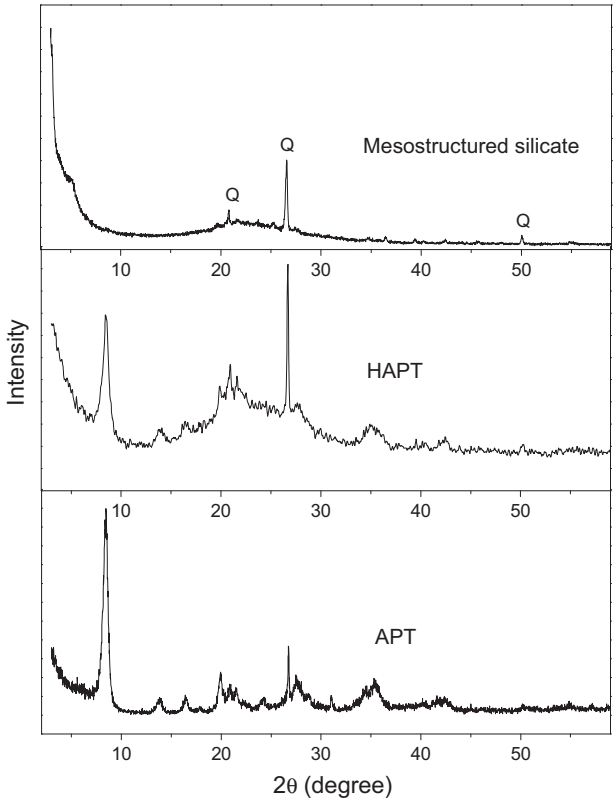

Fig. 1 Wide-angle X-ray diffraction profiles of APT, HAPT, and the calcined mesostructured silicate

(100) direction uniform square pattern of dots was observed though there was a locally uneven projection pattern due to misalignment, and along the (110) direction a regular monoclinic pattern of the channels was seen. Measurements of the distances between the pores on the observed planes indicated that the sample had a body-centered cubic structure [28, 29]. The results obtained in TEM for MCM-48-like silicate were consistent with that from XRD in Fig. 3. The SEM images illustrated the morphology of fragments of loose flakes for WHMS-like silicate (Fig. 4e) and MCM-48-like silicate had the shape in fine spherical particles similar to that previously reported (Fig. 4f) [30, 31]. The fiber-like structure for APT disappeared completely and a new morphology formed. Clearly, the acid-alkaline treatment process affected much on the mesostructure formation as well as the morphology. As for the new morphology formation it can be explained as below. First, APT was activated by con. HCl solution, resulting its crystallinity decreasing and most of the metals incorporated in the structure lost. This step made the crystalline structure of APT unstable. Then in the mesostructured silicates synthetic process it was under alkaline solution, which further dissolved the activated attapulgite. Because its main composition was silica, whose stable crystalline structure was destroyed by acid treatment, the activated attapulgite reconstructed by forming ordered mesostructured silicates in the presence of surfactants as

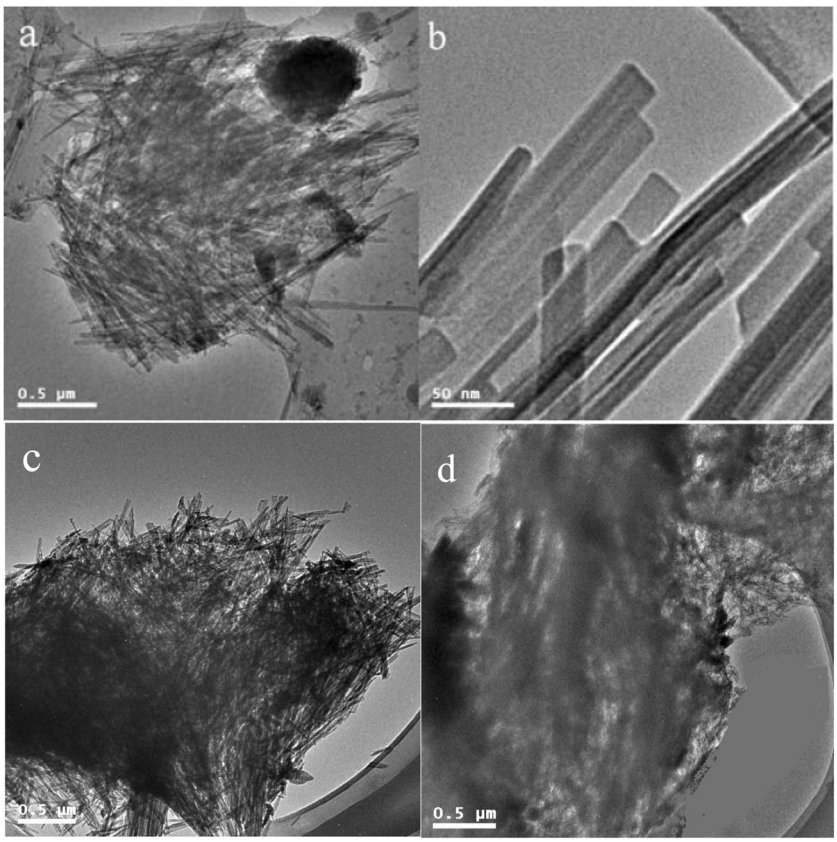

Fig. 2 TEM images for APT (**a**, **b**) and HAPT (**c**, **d**)

Table 2 Textural properties of mesoporous silicate materials synthesized from hydrothermal crystallization of CTAB/HAPT/H_2O/NaOH/ethanol systems under various pH values

Sample	pH of the gel	S_{BET} (m^2/g)	V_{pore} (cm^3/g)	D_{BJH} (nm)	mesophase
ATP	—	134	0.37	—	—
HATP	—	264	0.58	—	—
WHMS-like silicate	11.0	997	0.84	2.7	3D hexagonal
MCM-48-like silicate	11.5	810	0.43	2.3	Cubic
Lamellar silicate	12.0	401	0.39	—	Lamellar

template. As a result, the fiber-like morphology of attapulgite clay disappeared with the formation of a new morphology.

Anyway, by varying pH value in the synthetic stage, three ordered mesostructured silicates including cubic, 3D hexagonal, and lamellar phases, were successfully fabricated by using HAPT as raw material. The transformation of mesophases induced by controlling pH value has been observed in the literatures [32, 33].

The N_2 adsorption–desorption isotherms for APT, HAPT, MCM-48-like, WHMS-like, and lamellar silicates after calcination, were presented in Fig. 5 (left). And their corresponding textural properties are listed in Table 2. APT and HAPT had type II isotherms, while MCM-48-like and WHMS-like silicates exhibited isotherms of type IV, characteristic of mesoporous materials with well-defined uniform pore diameter. A shift of N_2 uptake step towards lower relative pressure from $P/P_0 = 0.26$–0.37 for WHMS-like silicate to 0.15–0.3 for MCM-48-like silicate, implying the decreasing tendency of their pore size. The hysteresis in the desorption isotherm featuring a sharp step has previously been ascribed to delayed capillary evaporation from (meso) pores with narrow constrictions [34, 35]. However, the isotherm of calcined lamellar silicate was of type II, indicating a highly non-uniform porous system, and a broad triangular H3 hysteresis loop was observed at medium to high partial pressure, suggesting the presence of disordered domains resulting from the collapse of lamellar structures. Eventhough, it is noteworthy that the calcined lamellar silicate had a quite considerable BET-specific surface area of about 401 m^2/g and a total pore volume of 0.39 cm^3/g. The corresponding BJH pore size distributions for calcined mesostructured silicates, with lamellar silicate and HAPT inserted, are shown in Fig. 5 (right). APT gave similar curve as that of HAPT, therefore, it was omitted. No peak for lamellar silicate and HAPT was observed, demonstrating their non-uniform porous system, which was consistent with the result from their type II adsorption–desorption isotherms.

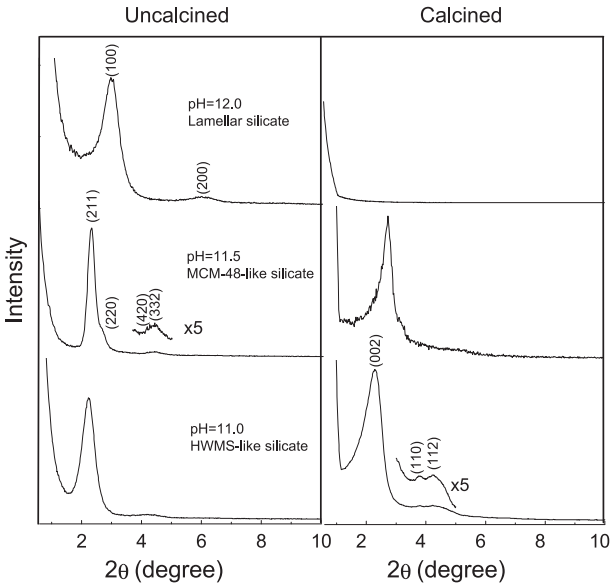

Fig. 3 Low-angle X-ray diffraction patterns of mesostructured silicate, uncalcined (left), and calcined (right).

MCM-48-like and WHMS-like silicates show narrow pore size distributions centered at 2.3 and 2.7 nm, respectively. The BET surface areas for MCM-48-like and WHMS-like silicates are 810 and 997 m^2/g, respectively, with their corresponding pore volume of 0.43 and 0.84 cm^3/g.

The FT-IR spectra in the range of 400–4000 cm^{-1} for mesoporous silicates and pure MCM-48 are shown in Fig. 6. All of the spectra showed a main band at 1080 cm^{-1} together with a shoulder at 1250 cm^{-1} ascribed to asymmetric Si–O–Si stretching modes. Also, a strong band at 800 cm^{-1} and a band at 463 cm^{-1} were assigned to Si–O–Si symmetric stretching mode and Si–O–Si rocking mode, respectively. It was obviously seen in spectra that the peak at 810 cm^{-1} became weak from siliceous MCM-48 to mesoporous silicates and the signal at 973 cm^{-1} was shifted towards lower wavenumber with its intensity stronger. It is noteworthy that the incorporation of metal into purely siliceous mesoporous materials caused an increase in intensity of the component assigned to the Si-(OH) stretching mode at 973 cm^{-1} [36, 37]. The increasing in intensity ratio of I973/I810 for mesoporous silicates in comparison with pure MCM-48 can be regarded as a proof for the incorporation of metal species into the mesoporous silicate framework prepared from HAPT [36, 38].

ICP technique was employed to detect the metal contents in the final mesostructure. The results were listed in Table 1. Clearly, the preserved metal contents of Al/Ti/Mg in the obtained mesostructured silicates were rather significant. What was interesting was that the incorporation of Al into the three mesoporous silicates was the same with the Si/Al molar ratio of 19, while the Mg and Ti contents were similar and depended on the type of mesophase, which was rather

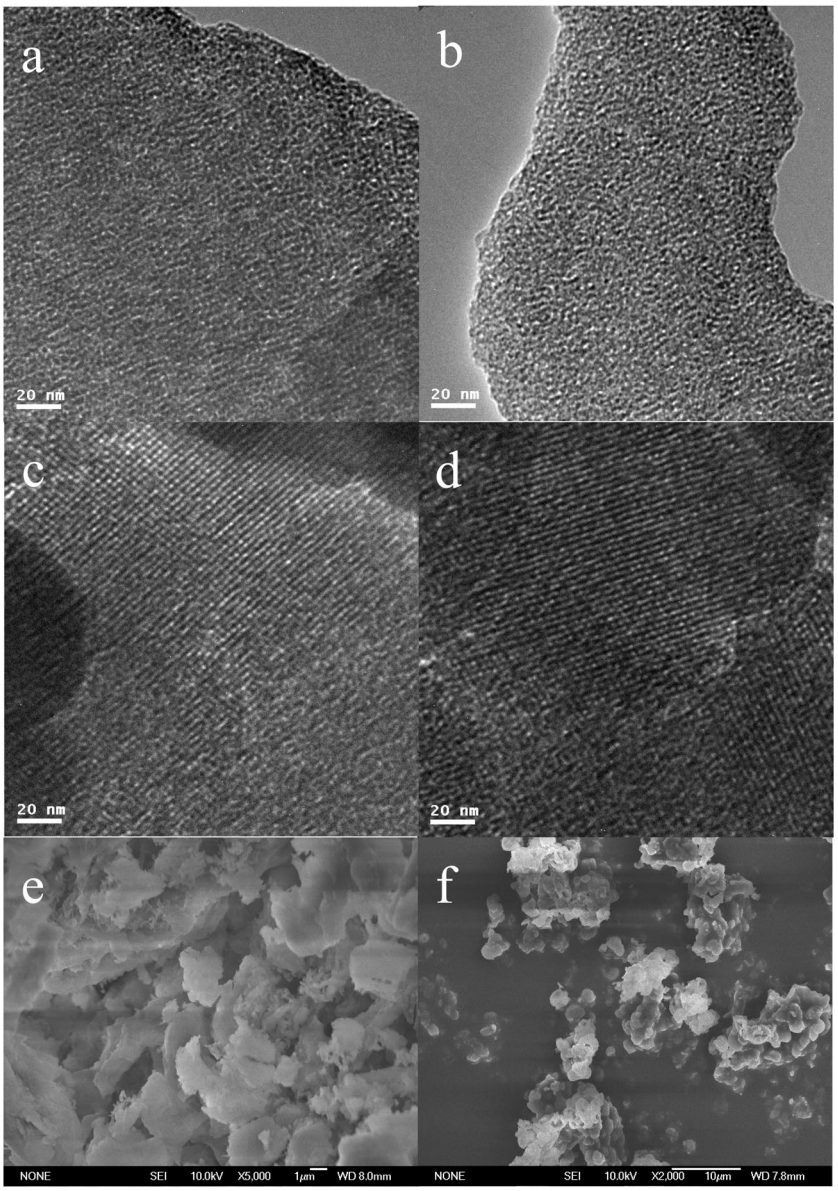

Fig. 4 TEM images of the calcined samples: **a**, **b** WHMS-like silicate, **c**,**d** MCM-48-like silicate along the axis of [100] and [110]. And SEM images of WHMS-like silicate (**e**) and MCM-48-like silicate (**f**)

desirable in MCM-48-like silicates but arid in lamellar and WHMS-like silicate. Anyway, the Al/Ti/Mg heteroatom contents in the three mesoporous silicates reached to the requirement for catalytic applications, such as the highly acidic MgAl-MCM-41 for the isopropylation of *m*-cresol with n_{Si}/n_{Al} in the 22–158 range and n_{Si}/n_{Mg} in the 24–154 range [17], and Ti-containing alkylated MCM-41 and MCM-48 with Si/Ti molar ratio in 77–138 range for the oxidation of cyclododecene [39]. Therefore, it is possible to apply these as-made mesostructured silicates with multiple metal cations for oxidative and acid-catalytic reactions.

To further confirm the accessibility of hetero-atoms in the pore surface, NH_3-TPD was conducted. Figure 7 gives the NH_3-TPD profiles for H-WHMS-like and H-MCM-48-like silicates as representatives. According to the ICP analysis that the Al content was much higher than the other metal content in the silicates, the surface acidity measured can be considered to be related with Al species. The ammonia desorption traces of both two samples were deconvoluted using Gaussian functions with temperature as variant. The first peak around 420−440 K referred to as type (i), which was attributed to surface (defect) or terminal hydroxyl groups (weak Brönsted acid sites), whereas the other two peaks, viz. types (ii) and (iii), in the range of 470 and 550 K were ascribed to moderate and strong (Brönsted) acid sites. The latter two may originate from the presence of trivalent aluminum in two different framework positions. The broad and weak peak around 620−700 K, designated as type (iv), was attributed to weak (structural) Lewis acid sites, which may arise from tri-coordinated aluminum in the

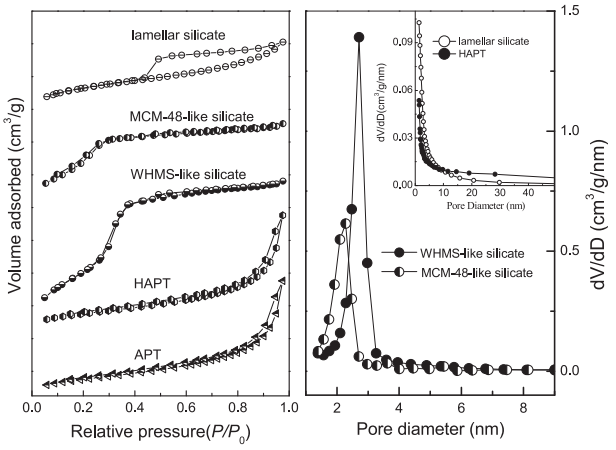

Fig. 5 N_2 adsorption and desorption isotherms of APT, HAPT, and calcined mesostructured silicates (left), with their corresponding pore size distributions (right)

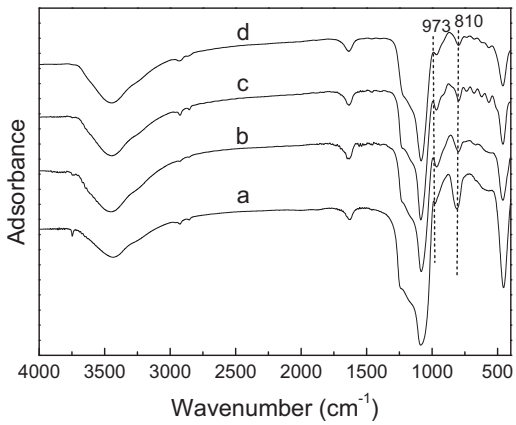

Fig. 6 FT-IR spectra of calcined samples: pure MCM-48 (**a**), WHMS-like silicate (**b**), MCM-48-like silicate (**c**), and lamellar silicate (**d**)

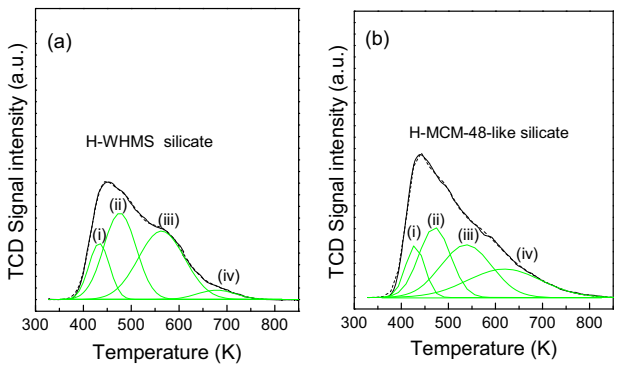

Fig. 7 NH_3-TPD profiles: (**a**) H-WHMS-like silicate; (**b**) H-MCM-48-like silicate

framework. The four types of acid sites in H-WHMS-like and H-MCM-48-like silicates also presented in H-AlMCM-41 materials synthesized with aluminum sulfate as Al sources [9, 40]. The NH_3-TPD analysis demonstrated the possibility of mesostructured silicates as heterogeneous catalyst for acid-catalytic reaction [9, 11, 40].

4 Conclusions

Aluminum/titanium/magnesium containing mesoporous silicates with cubic *Ia3d*, 3D hexagonal, and lamellar mesostructures, have been successfully synthesized via hydrothermal treatment of acid-leached attapulgite as precursor. Pretreatment of natural attapulgite with hydrochloric acid (4 M) under proper time and temperature was vital to activate the natural clay attapulgite and to keep adequate metal ions as sources for the synthesis of heteroatom-containing mesostructured silicates. ICP and FT-IR analyses illustrated the inclusion of metal species in the mesostructured silicates in precious amount. NH_3-TPD demonstrated the accessibility of Al species in the mesostructured framework located on the pore surface. All above indicated it could be an economical and environmentally friendly way to use those metal-doped mesoporous silicate with well-defined mesostructures prepared by using attapulgite as heterogeneous catalysts.

Acknowledgements This work was supported by the National Natural Science Foundation of China (No. 21503041).

Compliance with ethical standards

Conflict of interest The authors declare that they have no conflict of interest.

References

1. Zhou L, Liu X, Sun Y, Li J, Zhou Y (2005) Methane sorption in ordered mesoporous silica SBA-15 in the presence of water. J Phys Chem B 109:22710–22714
2. Kumar D, Schumacher K, Hohenesche CDF, Grun M, Unger KK (2001) MCM-41, MCM-48 and related mesoporous adsorbents: their synthesis and characterization. Colloids Surf A 187:109–116
3. Beck JS, Vartuli JC, Roth WJ, Leonowicz ME, Kresge CT, Schmitt KD, Chu CTW, Olson DH, Sheppard EW, McCullen SB, Huggins JB, Schlenker JL (1992) A new family of mesoporous molecular sieves prepared with liquid crystal templates. J Am Chem Soc 114:10834
4. Lee JW, Cho DL, Shim WG, Moon H (2004) Application of mesoporous MCM-48 and SBA-15 materials for the separation of biochemicals dissolved in aqueous solution. Kor J Chem Eng 21:246
5. Poh NE, Nur H, Nazlan M, Muhid M, Hamdan H (2006) Sulphated AlMCM-41: mesoporous solid Brønsted acid catalyst for dibenzoylation of biphenyl. Catal Today 114:257–262
6. Selvaraj M, Seshadri KS, Pandurangan A, Lee TG (2005) Highly selective synthesis of trans-stilbene oxide over mesoporous Mn-MCM-41 and Zr–Mn-MCM-41 molecular sieves. Micro Mesopor Mat 79:261–268

7. Fricke R, Kosslick H, Lischke G, Richter M (2000) Incorporation of gallium into zeolites: syntheses, properties and catalytic application. Chem Rev 100:2303
8. Kosslick H, Lischke G, Landmesser H, Parlitz B, Storek W, Fricke R (1998) Acidity and catalytic behavior of substituted MCM-48. J Catal 176:102
9. Sakthivel A, Badamali SK, Selvam P (2000) para-Selective t-butylation of phenol over mesoporous H-AlMCM-41. Micro Mesopor Mat 39:457
10. Morey MS, O'Brien S, Schwarz S, Stucky GD (2000) Hydrothermal and postsynthesis surface modification of cubic MCM-48, and ultralarge pore SBA-15 mesoporous silica with titanium. Chem Mater 12:898
11. Pu SB, Kim JB, Seno M, Inui MT (1997) Isopropylation of polynuclear aromatic hydrocarbons on Al-containing M41S mesoporous catalysts. Micro Mater 10:25
12. Iwanami K, Sakakura T, Yasuda H (2009) Efficient catalysis of mesoporous Al-MCM-41 for mukaiyama aldol reactions. Catal Commun 10:1990–1994
13. Choi JS, Yoon SS, Jang SH, Ahn WS (2006) Phenol hydroxylation using Fe-MCM-41 catalysts. Catal Today 111:280
14. Preethi MEL, Revathi S, Sivakumar T, Manikandan D, Divakar D, Rupa AV, Palanichami M (2008) Phenol hydroxylation using Fe/Al-MCM-41 catalysts. Catal Lett 120:56–64
15. Liu H, Lu GZ, Guo YL, Guo Y, Wang JS (2006) Synthesis of framework-substituted Fe-HMS and its catalytic performance for phenol hydroxylation. Nanotechnology 17:997
16. Timofeeva MN, Malyshev ME, Panchenko VN, Shmakov AN, Potapov AG, Mel'gunov MS (2010) $FeAl_{12}$-Keggin type cation as an active site source for Fe,Al-silica mesoporous catalysts. Appl Catal B: Environ 95:110–119
17. Vinu A, Ariga K, Saravanamurugan S, Hartmann M, Murugesan V (2004) Synthesis of highly acidic and well ordered MgAl-MCM-41 and its catalytic performance on the isopropylation of m-cresol. Micro Mesopor Mat 76:91–98
18. Jang HT, Park YK, Ko YS, Lee JY, Margandan B (2009) Highly siliceous MCM-48 from rice husk ash for CO_2 adsorption. Int J Greenh Gas Con 3:545
19. Kumar P, Mal N, Oumi Y, Yamana K, Sano T (2001) Mesoporous materials prepared using coal fly ash as the silicon and aluminium source. J Mater Chem 11:3285
20. Liu Y, Pinnavaia TJ (2004) Metakaolin as a reagent for the assembly of mesoporous aluminosilicates with hexagonal, cubic and wormhole framework structures from proto-faujasitic nanoclusters. J Mater Chem 14:3416–3420
21. Yang H, Tang D, Ouyang J, Li M, Mann S (2010) From natural attapulgite to mesoporous materials: methodology, characterization and structural evolution. J Phys Chem B 114:2390–2398
22. Eberl DD, Velde B, McCormick T (1993) Synthesis of illite-smectite from smectite at earth surface temperatures and high pH. Clay Miner 28:49–60
23. Rassineus F, Griffault L, Mcunier A, Berger G, Petit S, Vieillard P, Zellagui R, Munoz M (2001) Expandability-layer stacking relationship during experimental alteration of a Wyoming bentonite in pH 13.5 solutions at 35 and 60 °C. Clay Miner 36:197–210
24. Kim JM, Stucky GD (2000) Synthesis of highly ordered mesoporous silica materials using sodium silicate and amphiphilic block copolymers. Chem Commun 1159.
25. Christiansen SC, Zhao DY, Janicke MT, Landry CC, Stucky GD, Chmelka BF (2001) Molecularly ordered inorganic frameworks in layered silicate surfactant mesophases. J Am Chem Soc 123:4519
26. Wang LQ, Exarhos GJ (2003) Investigation of local molecular ordering in layered surfactant-silicate mesophase composites. J Phys Chem B 107:443
27. Schumacher K, von Hohenesche CD, Unger KK, Ulrich R, Chesne AD, Wiesner U, Spiess HW (1999) The synthesis of spherical mesoporous molecular sieves MCM-48 with heteroatoms incorporated into the silica framework. Adv Mater 11:1194
28. Schmidt R, Stöcker M, Akporiaye D, Torstad EH, Olsen A (1995) High-resolution electron microscopy and X-ray diffraction studies of MCM-48. Micro Mater 5:1
29. Yuan ZY, Luo Q, Liu JQ, Chen TH, Wang JZ, Li HX (2001) Synthesis and characterization of boron-containing MCM-48 cubic mesoporous molecular sieves. Micro Mesopor Mat 42:289
30. Wang KX, Lin YJ, Morrisa MA, Holmes JD (2006) Preparation of MCM-48 materials with enhanced hydrothermal stability. J Mater Chem 16:4051–4057
31. Endud S, Wong K (2007) Mesoporous silica MCM-48 molecular sieve modified with $SnCl_2$ in alkaline medium for selective oxidation of alcohol. Micro Mesopor Mat 101:256–263
32. Jin ZW, Wang XD, Cui XG (2007) Acidity-dependent mesostructure transformation of highly ordered mesoporous silica materials during a two-step synthesis. J Non-Cryst Solids 353:2507–2514
33. Boissière C, Larbot A, Van der Lee A, Kooyman PJ, Prouzet E (2000) A new synthesis of mesoporous MSU-X silica controlled by a two-step pathway. Chem Mat 12:2902–2913
34. Kruk M, Jaroniec M, Pena ML, Rey F (2002) Determination of phase composition of MCM-48/Lamellar phase mixtures using nitrogen adsorption and thermogravimetry. Chem Mater 14:4434
35. Hou Q, Margolese D, Stucky GD (1996) Surfactant control of phases in the synthesis of mesoporous silica-based materials. Chem Mater 8:1147
36. Ryoo R, Ko CH, Howe RF (1997) Imaging the distribution of framework aluminum in mesoporous molecular sieve MCM-41. Chem Mater 9:1607
37. Ricchiardi G, Damin A, Bordiga S, Lamberti C, Spano G, Rivetti F, Zecchina A (2001) Vibrational structure of titanium silicate catalysts. A spectroscopic and theoretical study. J Am Chem Soc 123:11409–11419
38. Shao YF, Wang LZ, Zhang JL, Anpo M (2005) Synthesis of hydrothermally stable and long-range ordered Ce-MCM-48 and Fe-MCM-48 materials. J Phys Chem B 109:20835–20841
39. Igarashi N, Hashimoto K, Tatsumi T (2007) Catalytical studies on trimethylsilylated Ti-MCM-41 and Ti-MCM-48 materials. Micro Mesopor Mat 104:269–280
40. Dapurkar SE, Selvam P (2003) Mesoporous H-AlMCM-48: highly efficient solid acid catalyst. Appl Catal A-Gen 254:239–249